2011 NDIA GROUND VEHICLE SYSTEMS ENGINEERING AND TECHNOLOGY SYMPOSIUM
MODELING & SIMULATION, TESTING AND VALIDATION (MSTV) MINI-SYMPOSIUM
AUGUST 9-11 DEARBORN, MICHIGAN

A USER-FRIENDLY TOOL FOR EVALUATING THE THERMAL RESPONSE OF HIGH POWER BATTERY PACKAGING ALTERNATIVES

Stanley Jones, PhD
Science Applications International Corporation
Evergreen, CO

John Mendoza, PhD
Science Applications International Corporation
El Segundo, CA

George Frazier
Science Applications International Corporation
Oakland, CA

Sonya Zanardelli
Tank-Automotive Research, Development Engineering Center
Warren, MI

ABSTRACT

The SAIC Battery Thermal Solver is a tool that allows for the evaluation of the thermal response under a variety of cell types, loading conditions and packaging alternatives for the battery designer, manufacturer, or system integrator. Developed with a user-friendly interface, the Battery Thermal Solver allows for a number of simulations to be performed. This paper discusses the capabilities of the Battery Thermal Solver Tool through a thorough discussion of the battery thermal problem—from cell heat generation, heat transfer mechanisms, to the effects of alternative packaging strategies.

INTRODUCTION

High power battery systems such as those used for hybrid vehicle tractive assist, silent watch functions and pulse power systems can experience large current demands. Waste heat generated under these large loading conditions can place a significant premium on heat removal mechanisms. This is particularly true as battery systems are subject to challenging environmental conditions and thermal management system dependencies in integrated military vehicle platforms. Battery systems need to be maintained below safe temperature limits and above extreme cold conditions. Typically in the form of arrays of cells packaged into structural modules to form a battery pack, the integrated design of a battery assembly needs to account for thermal maintenance of the assembly to ensure that adequate performance is maintained. Heat generated within the cell body must be transferred via conduction to the cell/module exterior where it is carried away via convection mechanisms to either an air or fluid coolant. The best possible packaging alternative can be a function of a number of factors including cell morphology and form factor, packaging structures, imposed demand, and integration interface requirements.

Detailed finite element simulations of battery structures can prove costly in terms of both time and effort. Complicating the cell heat transfer problem is the inherent anisotropic nature of thermal properties within the cell core. This problem is often compounded by uncertainties in input parameters such as material properties, heat transfer coefficients and heat generation rates. The SAIC Battery Thermal Solver utilizes a semi-analytical solution to solve the transient three-dimensional thermal problem rapidly on an ordinary personal computer. Further, the Battery Thermal Solver has an incorporated Monte Carlo simulator to allow for the propagation of parameter uncertainty and better characterize expected performance under a range of operating conditions.

MODELING DETAILS

Battery cell structures are typically either cylindrical or prismatic (rectilinear) in nature. The analysis demonstrated herein is the prismatic solution. Analogous solutions for cylindrical and annular structures are handled in a similar fashion. Cell tabbing, anode/cathode construction, cans or pouches and electrical isolation layers generate a variety of boundary conditions to the cell interior that go beyond this discussion but are accounted for through boundary condition designation.

The SAIC Battery Thermal Solver utilizes a closed-form solution for the temperature variation of the cell core.

Report Documentation Page

Form Approved
OMB No. 0704-0188

1. REPORT DATE	2. REPORT TYPE	3. DATES COVERED
09 AUG 2011	**N/A**	**-**

4. TITLE AND SUBTITLE	5a. CONTRACT NUMBER
A User-Friendly Tool for Evaluationg the Thermal Response of High Power Battery Packaging Alternatives	5b. GRANT NUMBER
	5c. PROGRAM ELEMENT NUMBER
6. AUTHOR(S)	5d. PROJECT NUMBER
Stanley Jones; John Mendoza; George Frazier; Sonya Zanardelli	5e. TASK NUMBER
	5f. WORK UNIT NUMBER
7. PERFORMING ORGANIZATION NAME(S) AND ADDRESS(ES)	8. PERFORMING ORGANIZATION REPORT NUMBER
US Army RDECOM-TARDEC 6501 E 11 Mile Rd Warren, MI 48397-5000, USA Science Applications International Corporation Evergreen, CO, USA Science Applications International Corporation El Segundo, CA, USA Science Applications International Corporation Oakland, CA, USA	**21997**
9. SPONSORING/MONITORING AGENCY NAME(S) AND ADDRESS(ES)	10. SPONSOR/MONITOR'S ACRONYM(S)
US Army RDECOM-TARDEC 6501 E 11 Mile Rd Warren, MI 48397-5000, USA	**TACOM/TARDEC/RDECOM**
	11. SPONSOR/MONITOR'S REPORT NUMBER(S) **21997**

12. DISTRIBUTION/AVAILABILITY STATEMENT
Approved for public release, distribution unlimited

13. SUPPLEMENTARY NOTES
Presented at the 2011 NDIA Vehicles Systems Engineering and Technology Symposium 9-11 August 2011, Dearborn, Michigan, USA, The original document contains color images.

14. ABSTRACT

15. SUBJECT TERMS

16. SECURITY CLASSIFICATION OF:			17. LIMITATION OF ABSTRACT	18. NUMBER OF PAGES	19a. NAME OF RESPONSIBLE PERSON
a. REPORT	b. ABSTRACT	c. THIS PAGE			
unclassified	**unclassified**	**unclassified**	**SAR**	**9**	

Careful derivation of boundary condition estimates (through effective overall external heat transfer coefficients) allow this solution to be used for a variety of cell structures and packaging scenarios.

The prismatic cell has a core structure in the form of a rectangular prism as illustrated in Figure 1. The desired solution is one of flexibility such that the aspect ratios of this structure and independent effective heat transfer coefficients on all six faces are user defined.

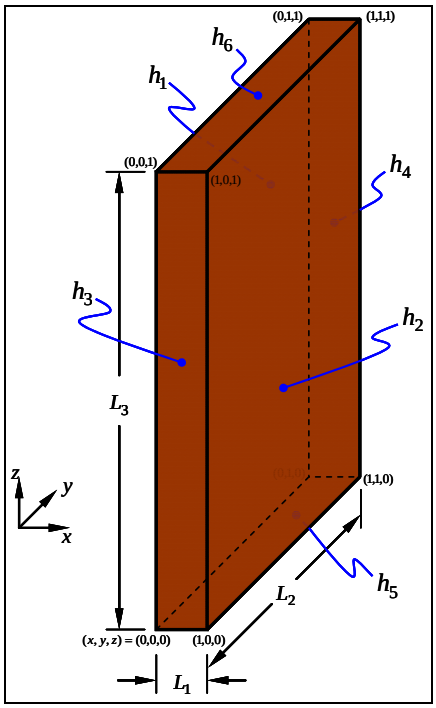

Figure 1: Prismatic Battery Core

The transient energy equation for a 3-D Cartesian solid with anisotropic (but constant) properties and a uniformly distributed time variant volumetric heat generation rate can be written as:

$$\rho c_p \frac{\partial T}{\partial t} = k_\perp \frac{\partial^2 T}{\partial x^2} + k_\parallel \frac{\partial^2 T}{\partial y^2} + k_\parallel \frac{\partial^2 T}{\partial z^2} + \dot{Q}_v(t) \qquad (1)$$

Note that the thermal conductivity, $k_\perp$, represents the cross-plane core thermal conductivity and, $k_\parallel$, represents the in-plane core thermal conductivity (i.e. – the x-coordinate is aligned as the cross-plane coordinate).

The aim is to find a solution that can be applied across a range of applications without a priori knowledge of the surface temperatures. The most functional form of this solution utilizes convective boundary conditions at each of the six faces:

$$\begin{aligned}
k_\perp \frac{\partial T}{\partial x}\bigg|_{x=0} &= h_1(T_1 - T_\infty) \quad , \quad -k_\perp \frac{\partial T}{\partial x}\bigg|_{x=L_1} = h_2(T_2 - T_\infty) \\
k_\parallel \frac{\partial T}{\partial y}\bigg|_{y=0} &= h_3(T_3 - T_\infty) \quad , \quad -k_\parallel \frac{\partial T}{\partial y}\bigg|_{y=L_2} = h_4(T_4 - T_\infty) \\
k_\parallel \frac{\partial T}{\partial z}\bigg|_{z=0} &= h_5(T_5 - T_\infty) \quad , \quad -k_\parallel \frac{\partial T}{\partial z}\bigg|_{z=L_3} = h_6(T_6 - T_\infty)
\end{aligned} \qquad (2)$$

These boundary conditions (third kind) represent the equivalence of the thermal conduction within the core to the thermal convection leaving the face. For an initial condition, the core is assumed to be initially at a uniform temperature equal to the surrounding temperature [i.e. – $T(t=0) = T_0$].

PRISMATIC CELL STEADY-STATE SOLVER

Before addressing the transient solution, it is informative to examine the steady-state solver which has been programmed with a user-friendly graphical user interface (GUI). The steady-state solution has been programmed to allow for investigations of heating rates, boundary conditions, material properties and packaging scenarios as depicted in Figure 2.

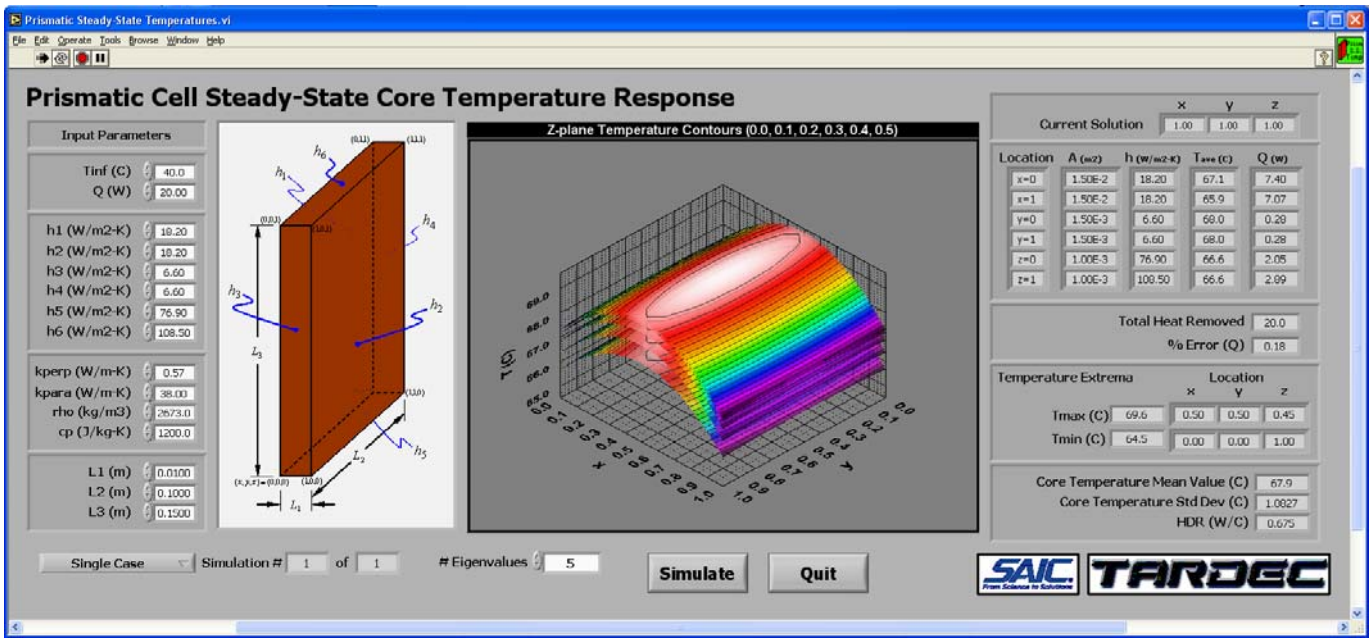

Figure 2: Prismatic Cell Steady-State Thermal Solver

The prismatic cell steady-state solver GUI allows for relatively straightforward calculations of temperature profiles generated from constant internal heat generation. To run a simulation, there are fifteen (15) required input parameters from four (4) separate classes:

- ***Problem Specifications****:* setting of the boundary condition temperature and cell heating rate
- ***Effective Heat Transfer Coefficients****:* measure of the thermal linkage between the battery core surfaces and the coolant temperature
- ***Battery Core Properties:*** includes effective values for the thermal conductivities (parallel, $k_{\parallel}$, and cross-plane, $k_{\perp}$), core density, and core specific heat
- ***Battery Core Dimensions:*** overall cell length, width, and height of the battery core

Heat Dissipation Rate

A key result from the steady-state solver is the heat dissipation rate (HDR). The HDR provides a quantifiable measure of the effectiveness of a particular packaging scheme and provides a useful measure for comparison between alternatives. It is defined as the quantity of heat generated within the cell divided by the difference between the maximum core temperature and the coolant temperature. Functionally it can be written as:

$$HDR = \frac{\dot{Q}}{T_{Max} - T_{Coolant}} \qquad (3)$$

The HDR provides a means for evaluating a battery package cooling strategy and a comparable measure between approaches. Heat dissipation rate is a function of the particular packaging strategy. Overall, a battery package cooling strategy may be air-cooled or water-cooled, but internal structures can play a significant role. Assemblies internal to a battery pack can often provide for or inhibit thermal conduction pathways and convection access. The HDR provides a measure to compare the overall thermal performance of a particular packaging approach.

If the HDR is low, this represents a package that must have a high allowable maximum temperature, have a very low coolant temperature, or be limited by the allowable quantity of heat generation. Alternatively, a high HDR package will allow for greater internal heating rate without violating the maximum cell internal temperature. It is the 'hot-spot' maximum temperature (T_{Max}) that the user must avoid to ensure battery longevity. If the HDR and maximum allowable cell temperature are known for a particular package, the system integrator can specify allowable coolant temperatures and cell demand limitations.

Exemplar Solutions

Several case studies were performed to help validate the solver. The expected results are given in the following figures. Figure 3 shows the temperature contours for a cell with uniform heat transfer coefficients on all six faces from an oblique perspective and a top-down view. Figure 4

shows a case with adiabatic conditions imposed along one face (x = 0). Similarly, a case with a y-axis adiabatic surface (y = 0) was solved; the results are shown in Figure 5. Lastly, a solution with two adiabatic surfaces is depicted in Figure 6.

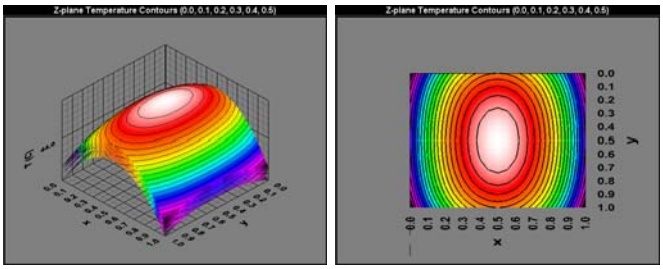

Figure 3: Temperature Contours with Uniform External Heat Transfer Coefficients

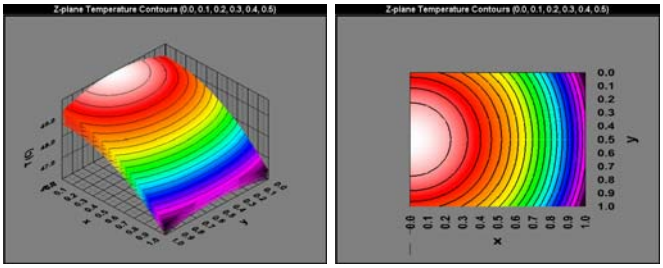

Figure 4: Temperature Contours with Adiabatic Conditions Imposed Along X=0 Face

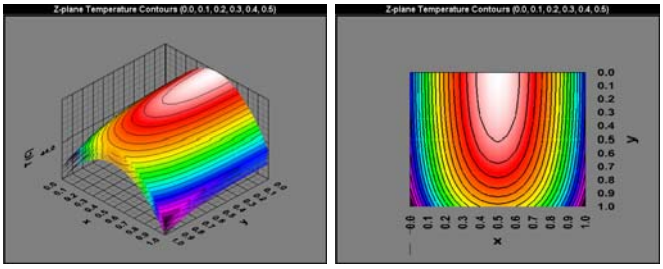

Figure 5: Temperature Contours with Adiabatic Conditions Imposed Along Y=0 Face

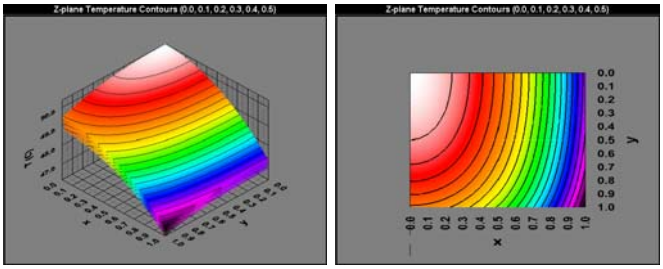

Figure 6: Temperature Contours with Adiabatic Conditions along X=0 & Y=0 Faces

The utility of the prismatic cell steady-state solver code is exemplified in an investigation of a packaging structure utilizing liquid-cooled cold plates. For this case, the cell package structure uses two coolant-fed cold plate structures above and below an array of prismatic cells. A simplified depiction of such a packaging structure is shown in Figure 7. Shown in cross-section, the cell array (three cells are shown) are sandwiched vertically between the two cold plates and laterally with adjacent cells. Within the interstitial regions between adjacent cells, an aluminum conduction fin provides necessary mechanical compression and a heat pathway to the cold plate structures. The cores themselves are assumed to be housed in an insulating pouch and additional insulating layers/air gaps have been assumed to exist between the upper and lower cell surfaces, busbar structures, and cold plates.

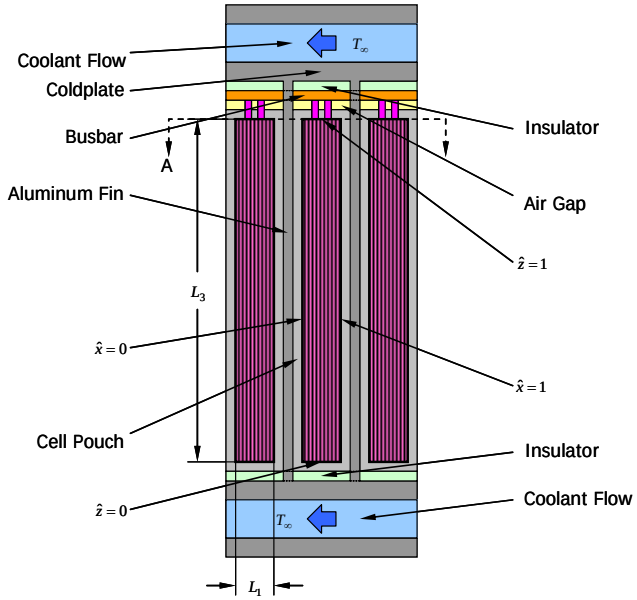

Figure 7: Prismatic Cell Array Packaged Between Cold Plates

A careful auditing of a proposed battery module structure and subsequent derivation of effective heat transfer coefficients is needed to generate reliable estimates of thermal performance. A thermal resistance derivation will usually suffice for the determination of effective heat transfer coefficients. For series-connected thermal resistances, such a calculation can typically be performed (for convective and conductive pathways in rectilinear systems) from a relation such as:

$$\frac{1}{h_{eff} A} = \sum_n \frac{1}{h_n A_n} + \sum_m \frac{\Delta x}{k_m A_m} \qquad (4)$$

Individual parameters in this expression are evaluated from the geometrical configurations, material properties and accepted heat transfer correlations. Parallel-connected heat transfer pathways and cylindrical structures can be treated in a similar fashion using the appropriate corresponding expressions.

Monte Carlo Simulator

A complete knowledge of the solver input parameters is difficult to know with absolute certainty. Utilizing a careful estimation of the effective heat transfer coefficients and best estimate for the core thermal properties is warranted, but there is still a good deal of parameter uncertainty. To get around this difficulty, a Monte Carlo simulator was coupled to the solver.

In a Monte Carlo simulation, each parameter is assigned a distribution of values that represents, to the best of the user's knowledge, the range and character of expected parameter values. The simulation draws randomly from these underlying distributions to generate simulation values. Repeated iterations of this process allow the user to generate best estimates (mean values) and uncertainty bands regarding the code estimates.

Through the Monte Carlo input parameter distribution window, the user can specify the distributions for each of the fifteen (15) input parameters. Three distribution types are currently allowed: Gaussian (normal) distributions, log-normal distributions and uniform distributions. Gaussian or normal distributions are used for parameter values that are relatively well known with an underlying uncertainty that is symmetrical about the mean value. Log-normal distributions are skewed to the positive above the mean and are often used with lesser known variables or in cases where negative parameters are not allowed. Uniform distributions are used when only an upper and lower parameter bound can be established. The tools at the bottom of this figure allow for the user to graphically depict any input parameter distribution prior to beginning the Monte Carlo simulation.

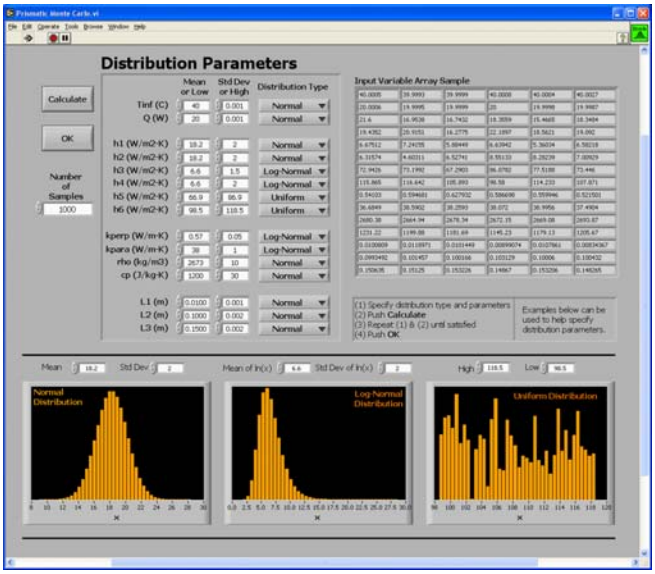

Figure 8: Distribution Parameter Specification for a Monte Carlo Simulation

A closer look at the parameter distribution section of the Monte Carlo set-up window for the cold plate cooling approach is shown in Figure 8. The user is allowed to select distributions and ranges (or distribution parameters) for boundary conditions, cell heating rate, boundary conditions, cell properties and dimensions. Distribution selection and definition is a function of the state-of-knowledge of the underlying parameter and may be based upon empirical evidence or engineering judgment.

When the solver executes, it samples from these distributions to come up with estimates of the expected mean value and a range of expected outcomes. After the execution a set of parameter distribution plots is displayed to the user as seen in Figure 9. Shown in the figure are the results of a 1000-point Monte Carlo sampling from the input parameter distributions.

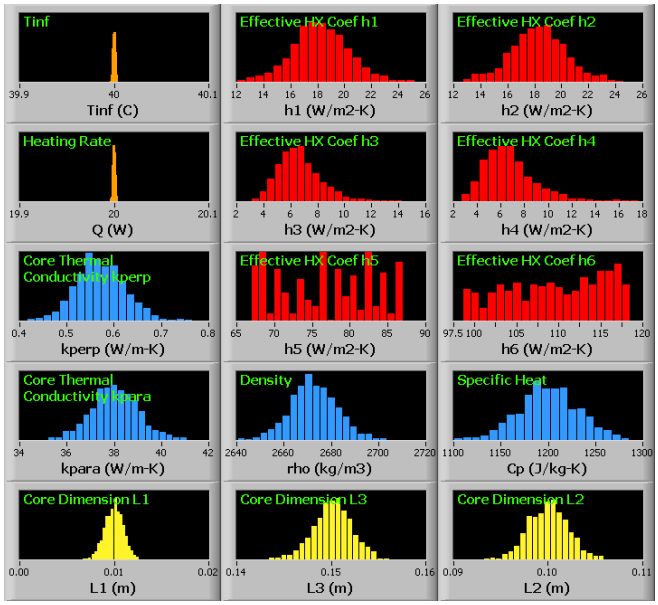

Figure 9: Input Parameter Distributions

After the Monte Carlo simulator completes the set of simulations, an internal post-processing of the results occurs and a window opens to show the results. Figure 10 presents the temperature distributions (minimum, average, and maximum core temperatures) for the cold plate cooling approach simulation while Figure 11 shows the HDR distribution for the setup.

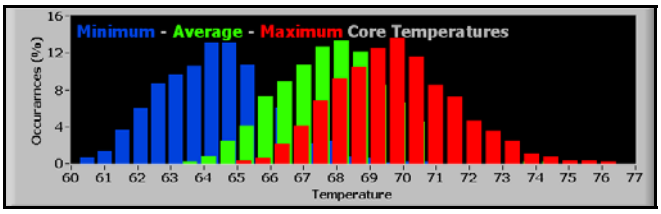

Figure 10: Battery Core Temperature Distribution Results

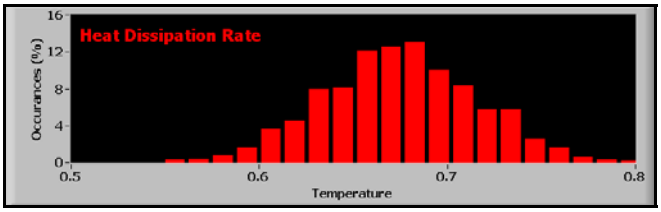

Figure 11: Heat Dissipation Rate Distribution

The utility of the results can be illustrated by looking at how the expected temperature difference from the cell core to the coolant can be estimated as a function of cell heating rate as shown in Figure 12. The expected maximum core temperature (shown in solid red) along with the uncertainty bounds of ±3σ (red shading). The minimum expected core temperature is also shown in blue.

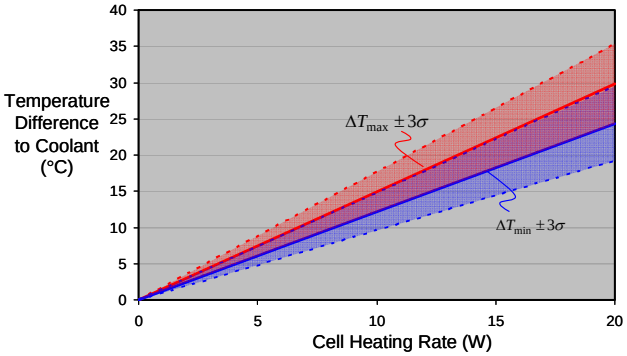

Figure 12: Cell Temperature Response to Heating Rate with Uncertainty Bands

Figure 12 demonstrates a direct use of the HDR to illustrate functional operation limits (HDR is the inverse of the slope of the depicted lines) of the cooling approach. If we were to consider a candidate cell in this packaging scheme with a maximum allowable temperature limit of 65°C and an expected cell heating rate of 10W. Safe operation of this cell would dictate that the coolant temperature cannot exceed 47°C (18°C difference to coolant) with no additional safety margin. To add additional safety margin, one would need to either maintain lower coolant temperatures or reduce the imposed cell current loading.

PRISMATIC CELL TRANSIENT SOLVER

The prismatic cell transient solver is an, as yet, independent solver that allows for the estimation of battery cell temperature response as a function of time-variant heating profiles. Three example cases are included here to demonstrate the solver performance and utility. Similar in set-up and GUI to the steady-state solver, the transient solver shown in Figure 13 has the same set of input parameters (effective boundary conditions, core thermal properties and cell dimensions) but includes the ability to load a transient heating file (delimited text format). The front end also has the ability to adjust the cell initial temperature, coolant temperature, and time parameters (step size and duration).

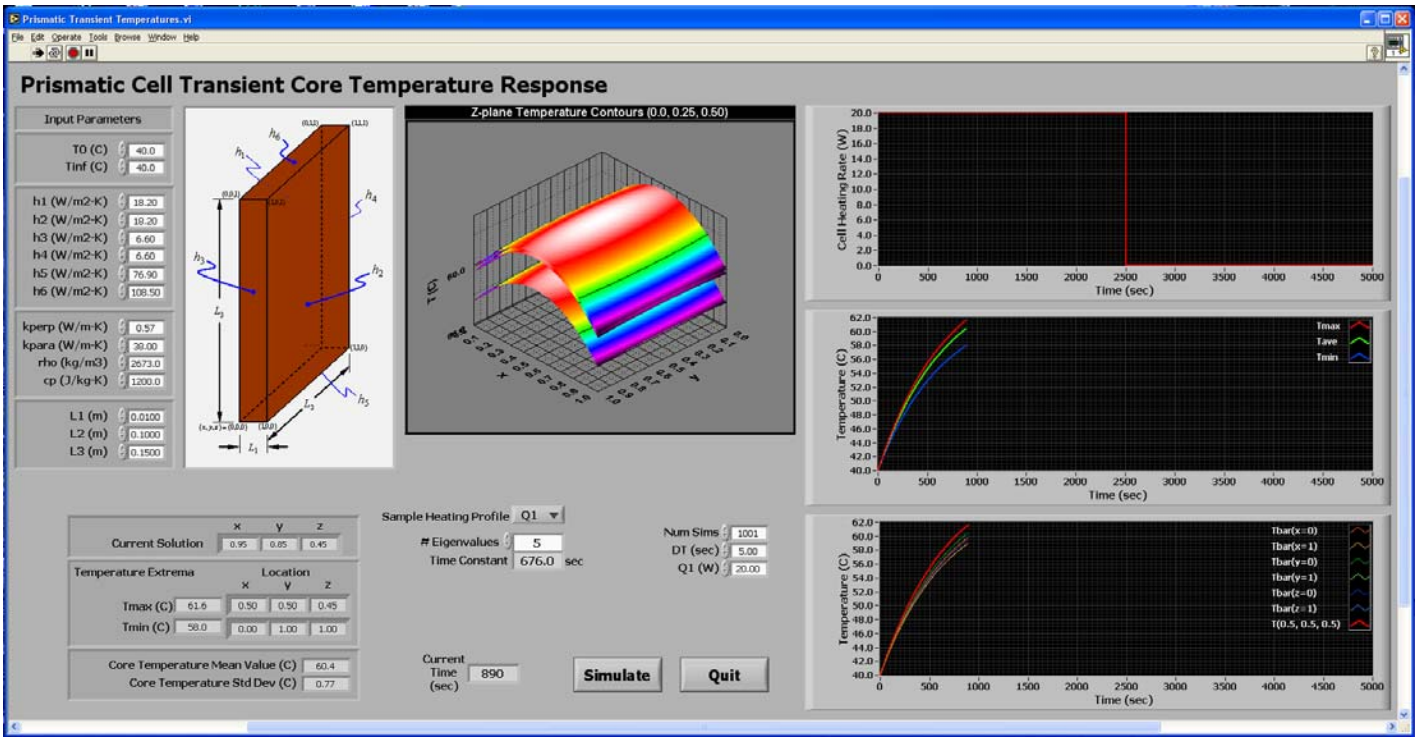

Figure 13: Prismatic Cell Transient Solver GUI

Currently, there are a couple of short-comings to the transient solver that should be mentioned. First, the solver currently has no means to account for a time-variant coolant temperature. However, provisions to allow for coolant temperature variation are in-process. The second shortcoming of the transient response model is an inability to account for the thermal inertia of the surrounding packaging structures. The components external to the battery cell that comprise the overall package (mounting, busbars, etc.) also undergo a transient temperature response. Time-variant boundary conditions have been identified as a means to rectify this shortcoming.

Three transient case studies have been studied to exemplify the operation of the transient model for the liquid-cooled cold plate, prismatic-cell package. The first example is a step change in heating response to demonstrate the transient heat up and subsequent temperature recovery after heat is removed. The second example is a continuous charge-discharge scenario representative of typically load-leveling operations. For the final example, a realistic driving scenario using transient empirical heating results from another study is simulated.

Step Change Heating

The step heating scenario is used to establish the temperature response of the cell to continuous loading followed by unloading to establish the time-constants of a particular battery packaging scenario. The heating rate profile is shown in Figure 14. For this particular example, a cell heating rate of 20W is applied to a cell for 2500 seconds. The battery cell is assumed initially at 40°C and the coolant is maintained at 40°C.

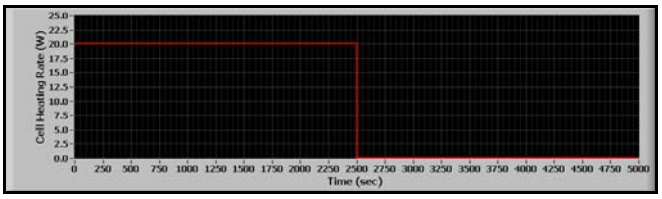

Figure 14: Step-Change Cell Heating Rate

The cell transient temperature response for the cold plate cooling approach is shown in Figure 15. Shown are maximum, average, and minimum cell temperatures. Note the expected exponential response of the battery temperatures to the imposed heating. The transient thermal solver calculates the time-constant of this packaging scenario (from the package-specific eigenvalues) and gives an answer of 676.0 seconds.

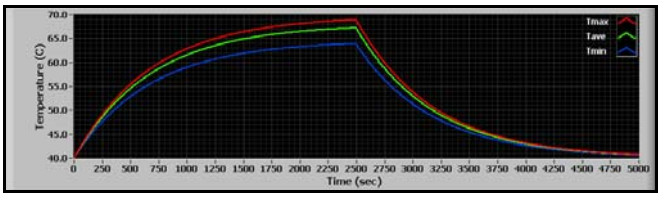

Figure 15: Cold Plate Cooling Approach Transient Thermal Response to Step-Change Heating

This simulation illustrates not only the warm-up time of the battery assembly but the amount of time required for thermal recovery after significant operations. It should be noted that the external thermal mass of packaging structures and system coolant has not been taken into account and therefore the actual packaging time constant could be substantially higher.

Successive Charge – Discharge

The successive charge-discharge scenario is one that represents a maximum continuous loading on a battery pack. For this example, a 100 A/cell discharge current is executed for 60 seconds followed by a 50 A/cell charge current for 120 seconds. In the simulation, this charge-discharge process was repeated for seven cycles. The heating profile predicted from a separate electro-thermal model (SAIC developed) was used as input to the thermal solver. The effect of the different heat rates between charge and discharge cycle is evident. In each simulation, the net effect on battery temperature is observed as a decrease during the charge cycle (Figure 16). Waste heat is still being fed into the battery core but at a substantially reduced rate.

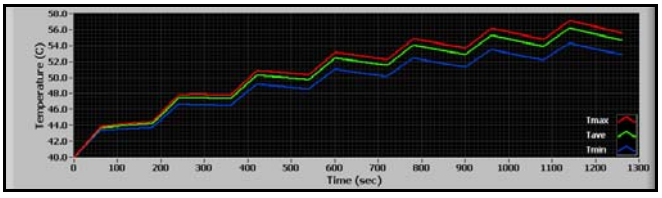

Figure 16: Cold Plate Cooling Approach Transient Thermal Response to Successive Charge-Discharge Heating Cycles

This solution demonstrates an overall exponential behavior as the cell structures eventually attain a quasi-steady state transient response to the imposed load-leveling cycles.

Realistic Driving Scenarios

A realistic driving scenario has also been simulated to further illustrate the utility of the code. This simulation utilizes actual field data from battery loading profiles in an off-road experiment. As before, time-based electrical loading data (current demand as a function of time) was fed to the electro-thermal model to generate a heating rate as a function of time. The derived heating rate for the driving scenario is shown in Figure 17. It is representative of actual driving conditions for an electric or hybrid vehicle mobility battery. Realistic battery loading are the result of rapidly changing response to acceleration demands, road obstacles, and vehicle energy management.

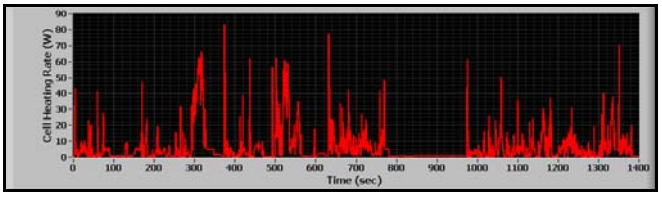

Figure 17: Off-Road Driving Profile #1 Battery Cell Heating Rate

The Battery Thermal Solver result for a cold plate cooling approach simulation using this heating profile with a 40°C initial temperature and a 40°C coolant temperature is shown in Figure 18. If one were to ignore the temperature-dependent property effects, the temperatures depicted in this figure can be translated up or down as a function of initial battery and coolant temperatures. More specifically, the predicted temperature differences can be roughly translated to hypothesize different initial conditions. For example, if the coolant and initial battery temperatures were at 60°C, this simulation predicts that a battery upper temperature limit of 65°C would be violated approximately 380 seconds into this simulation (ΔT = 5°C). This would imply that the vehicle battery management system would need to actively de-rate the available battery power to avoid overheating the cells.

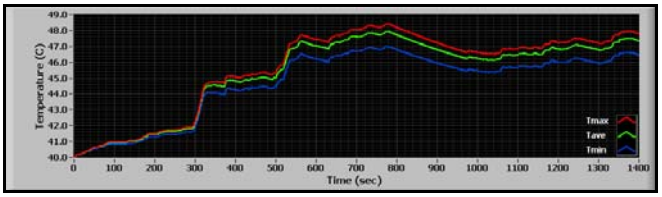

Figure 18: Cold-Plate Cooling Approach Transient Thermal Response to Off-Road Driving Profile #1

CONCLUSIONS

The SAIC Battery Thermal Solver suite of tools allow for the rapid evaluation of packaging alternatives, loading variations and changes to thermal boundary conditions. The solver allows for estimation of internal battery core thermal response avoiding costly and time consuming finite-element or empirical studies. Propagation of uncertainties present in cell properties, packaging structures, boundary conditions

and loading scenarios is addressed through an integrated Monte Carlo simulation tool.

The utility and user-friendliness of the SAIC Battery Thermal Solver have been demonstrated via steady-state and transient examples. Using the model, a quick evaluation of a liquid cooled cold-plate packaging approach was completed to determine its impact on the steady-state battery pack safe operational limits. Furthermore, the transient version of the code enabled an evaluation of the same packaging approach applied to the time-variant battery demands imposed in a realistic driving scenario.

Presently, only the prismatic version of the Battery Thermal Solver has been discussed. Similar solver tools for cylindrical and annular cell structures exist, but are, as yet, to be integrated in a single comprehensive suite of software tools. General tools to provide user guidance for boundary condition definition, transient coolant temperatures, temperature dependent properties and external package thermal inertia are envisioned.